Functional screen of MSI2 interactors identifies an essential role for SYNCRIP in myeloid leukemia stem cells

Ly P. Vu[1], Camila Prieto[1], Elianna M. Amin[1], Sagar Chhangawala[2,3], Andrei Krivtsov[4,5], M. Nieves Calvo-Vidal[6], Timothy Chou[1], Arthur Chow[1], Gerard Minuesa[1], Sun Mi Park[1], Trevor S. Barlowe[1], James Taggart[1], Patrick Tivnan[1], Raquel P. Deering[7], Lisa P Chu[8], Jeong-Ah Kwon[9], Cem Meydan[10], Javier Perales-Paton[11], Arora Arshi[12], Mithat Gönen[12], Christopher Famulare[13], Minal Patel[13], Elisabeth Paietta[14], Martin S. Tallman[15], Yuheng Lu[2], Jacob Glass[15], Francine Garret-Bakelman[16], Ari Melnick[17], Ross Levine[13], Fatima Al-Shahrour[11], Marcus Järås[18], Nir Hacohen[7], Alexia Hwang[19], Ralph Garippa[19], Christopher J. Lengner[20], Scott A Armstrong[4,5], Leandro Cerchietti[5], Glenn S Cowley[21], David Root[22], John Doench[22], Christina Leslie[2], Benjamin L Ebert[8], and Michael G. Kharas[1,*]

[1]Molecular Pharmacology Program, Center for Cell Engineering, Center for Stem Cell Biology, Center for Experimental Therapeutics, Memorial Sloan Kettering Cancer Center, New York, NY

[2]Computational Biology Program Memorial Sloan Kettering Cancer Center, New York NY

[3]Physiology Biophysics and Systems Biology Graduate Program, Weill Cornell Graduate School of Medical Sciences, Cornell University, New York, NY

[4]Cancer Biology and Genetics Program Memorial Sloan Kettering Cancer Center, New York, NY

[5]Department of Pediatric Oncology, Dana-Farber Cancer Institute, Harvard Medical School, Boston, MA

[6]Department of Medicine, Division of Hematology/Oncology, Weill Cornell Medical College, New York, NY

[7]Harvard Medical School, Boston, MA

[8]Brigham and Woman's Hospital, Division of Hematology, Boston, MA

[9]Whitehead Institute, Boston MA

[10]Institute for Computational Biomedicine, Department of Physiology and Biophysics, Weill Cornell Medical College, New York, NY

[11]Translational Bioinformatics Unit, Clinical Research Programme, Spanish National Cancer Research Centre, E-28029 Madrid, Spain

[12]Department of Epidemiology and Biostatistics, Memorial Sloan Kettering Cancer Center, New York, NY

[13]Human Oncology and Pathogenesis Program, Leukemia Service, Department of Medicine, Memorial Sloan Kettering Cancer Center, New York, NY

[14]Montefiore Medical Center, Bronx, NY

[15]Leukemia Service, Department of Medicine, Memorial Sloan Kettering Hospital; New York, NY

[16]Department of Medicine, University of Virginia, Charlottesville, VA; Department of Biochemistry and Molecular Genetics, University of Virginia, Charlottesville, VA

[17]Division of Hematology and Medical Oncology, Department of Medicine and Department of Pharmacology, Weill Cornell Medical College, Cornell University, New York, NY

[18]Department of Clinical Genetics, Lund University, Lund 22184, Sweden

[19]RNAi core, Memorial Sloan Kettering Cancer Center, New York, NY

[20]Department of Animal Biology, Department of Cell and Developmental Biology and Institute for Regenerative Medicine, Schools of Veterinary Medicine and Medicine, University of Pennsylvania, Philadelphia, PA

[21]Discovery Sciences, Janssen Research and Development, Welsh and McKean Roads, Spring House, PA

[22]Broad Institute, Boston MA

Abstract

The identity of the RNA binding proteins (RBPs) that govern cancer stem cell remains poorly characterized. The MSI2 RBP is a central regulator of translation of cancer stem cell programs. Through proteomics analysis of the MSI2 interacting RBP network and functional shRNA screening, we identified 24 genes required for *in vivo* leukemia and SYNCRIP was the most differentially required gene between normal and myeloid leukemia cells. SYNCRIP depletion increased apoptosis and differentiation while delaying leukemogenesis. Gene expression profiling of SYNCRIP depleted cells demonstrated a loss of the MLL and HOXA9 leukemia stem cell gene associated program. SYNCRIP and MSI2 interact indirectly though shared mRNA targets. SYNCRIP maintains HOXA9 translation and MSI2 or HOXA9 overexpression rescued the effects of SYNCRIP depletion. We validated SYNCRIP as a novel RBP that controls the myeloid leukemia stem cell program and propose that targeting these functional complexes might provide a novel therapeutic strategy in leukemia.

Acute myeloid leukemia (AML) is a genetically complex and heterogeneous set of diseases characterized by diverse set of mutations[1]. Despite an increased understanding of the molecular basis of AML pathogenesis, overall survival of adult AML patients has only improved modestly in the past 30 years[2]. Leukemia stem cells (LSCs) are a subpopulation characterized by a self-renewal capacity and an ability to recapitulate the phenotypic heterogeneity of the disease[3,4]. While somatic alterations in genetic and epigenetic mechanisms in leukemogenesis are intensively studied, how post-transcriptional and translational regulation of mRNA/protein expression impacts leukemia progression and leukemia stem cell (LSC) function remain poorly defined. Post-transcriptional regulation provides abundance and diversity of the proteome that can contribute to cell fate decisions. RNA binding proteins (RBPs) are the central arbiters of this complex regulatory process. Recently, RBPs have emerged as an important class of gene expression regulators in cancer and hematological malignancies[5,6]. Mutations in proteins involved in RNA processing and metabolism[7] such as DKC1[8], RPS19[9], and splicing factors[10,11] have been shown to contribute to hematologic diseases. Aberrant expression of several RBPs has been found in leukemia. For example, increased MSI2 RBP expression predicts a poor prognosis and drives the aggressiveness of leukemia[12–14]. MSI2 enhances translation of a number of critical genes (including c-*Myc*, *Hoxa9*, and *Ikzf2)* that are required for self-renewal of MLL-AF9 transformed leukemia stem cells (LSCs)[15,16]. While RBPs are thought to be abundant in multiple cell types, only a small fraction of RBPs have been functionally studied. As post-transcriptional regulation provides an additional level of control that dictates cell fate and cancer progression, understanding how RBPs control leukemia progression may result in the identification of novel targets in leukemia. In this study, we utilized an *in vivo* shRNA screening approach to functionally interrogate MSI2 associated RBP network to uncover novel regulatory factors important in leukemia.

Results

Pooled *in vivo* shRNA screening of the MSI2 interactome identified novel regulators of leukemia

In order to understand which RBPs are required for the survival of myeloid leukemia, we conducted an *in vivo* pooled short hairpin (shRNAs) screen in MLL-AF9 driven leukemia cells enriched for LSCs. The mixed lineage leukemia (MLL) gene has been shown to involved chromosomal translocations in over 70% of childhood leukemia and 5–10% of leukemia in adult[17].

T(9;11) MLL-AF9 translocation is the most common translocation in AML. Expression of the fusion protein MLL-AF9 in granulocyte-monocyte progenitor cells (GMPs) results in an established, robust, and short latency leukemia model, where LSCs can be enriched after serial transplantations[18,19]. Using the same leukemia model, we previously found that MSI2 function is required for self-renewal of LSCs[15]. Thus, to establish a relevant interacting riboproteomic network, we utilized MSI2 as a founding factor and performed mass spectrometry analysis of FLAG-MSI2 immunoprecipitated complexes in a leukemia cell line (K562) (Supplementary Fig.1a). A group of 234 proteins of multiple RBP classes were identified in association with MSI2 (Fig. 1a and Supplementary Table 1). Functional GO

term analysis linked these 234 proteins to RNA binding functions, including polyA binding and helicase activity (Supplementary Fig. 1b). To obtain a comprehensive assessment of MSI2 functional networks, we also utilized data generated from our MSI2 associated genomic studies to prioritize genes in different candidate pools for functional screening. 51 genes with differential expression found in MSI2 depleted CML/AML cell lines, MSI2 overexpressing LSK cells[12], and MSI2 KO LSK cells[15] were prioritized based on their associations with hematopoietic/leukemic gene sets (Supplementary Table 2), and Gene set enrichment analysis leading edge genes were included in pool 1 (Supplementary Table 3–4). Genes identified as MSI1 binding mRNA targets (Supplementary Table 5) were ranked and evaluated for their relevance to MSI2 and hematopoietic system, and 19 genes were included in pool 2 (Supplementary Table 6). Similarly, 58 genes discovered from MSI2 protein-protein interactions and had relevance to hematopoietic/leukemic gene sets were selected for pool 3 (Supplementary Table 7).

In total, we curated a list of 128 genes (Supplementary Table 8) and obtained 5–7 hairpins targeting each gene. Using a pooled library of titered shRNAs lentiviruses, we transduced sorted LSC enriched cells (a tertiary transplant of c-kit enriched MLL-AF9-dsRed leukemia) and subsequently transplanted them into sub lethally irradiated recipient mice (Fig. 1b). We allowed cells to engraft and then quantified the relative representation of each shRNA in the leukemia cells from the bone marrow and spleen at day 0 and day 16 post transplantation (Supplementary Table 9). We ultimately recovered a pool of shRNAs with greater than 20 fold depletion, which indicated a strong selection against their expression during leukemia progression (Fig.1c and Supplementary Fig. 1c–f). We prioritized the 24 top hits; each hit had at least five hairpins for that gave 20-fold depletion in both the bone marrow and spleen (Fig. 1d–e and Supplementary Table 10). GO analysis of the top genes revealed a significant enrichment for RBPs and mRNA binding proteins. The majority of the hits (20/24) were in the MSI2-protein-protein interaction group (Pool 3), suggesting that these complexes were important for disease progression (Fig. 1f–g). Among the top 24 scored genes, we selected seven genes (of which four encode RBPs) for in vitro validation including: *Syncrip*, *Caprin*, *Dyrk2*, *Hnrnpr*, *Cct3*, *Mybbp1*, and *Hnrnpa3* (Fig.1h and Supplementary Fig. 1g). In all of the genes tested, we confirmed knock down and observed a reduction in colony formation (Fig. 1i and Supplementary Fig. 1h). Additionally, MLL-AF9 leukemia cells were generally more sensitive to shRNA depletion compared to normal cells (c-kit+ enriched from bone marrow), except for *Dyrk2*, which was equally depleted (Fig. 1i). These data suggest a dysregulated RBP network is differentially required for leukemia cell survival compared to normal cells.

SYNCRIP is required for survival of leukemia cells

Of these in vitro validated genes, *SYNCRIP* demonstrated the most differential effect (10-fold) in colony forming ability between leukemia cells and normal c-kit+ enriched cells. Thus, we focused our investigation on SYNCRIP (*Syn*aptotagmin-binding, *c*ytoplasmic *R*NA-*i*nteracting *p*rotein; also known as NSAP1 or hnRNPQ1 in human), which has three tandem RNA recognition motifs and is implicated in regulation of RNA processing, transcript turnover, and protein translation[20–23]. Several studies suggest that SYNCRIP may have a role in neuronal morphogenesis[24,25]. Yet, the role for SYNCRIP in cancer or

leukemia has not been studied. To further evaluate the effects of SYNCRIP depletion, we first confirmed that shRNAs specific for *Syncrip* resulted in the reduction of SYNCRIP by immunoblot in MLL-AF9 transformed leukemia cells (Fig. 2a and Supplementary Fig. 2a). SYNCRIP depletion in leukemic cells resulted in rapid increase in myeloid differentiation based on increased Gr-1 and Mac-1, F480 and CD115 surface staining (Fig. 2b–c and Supplementary Fig. 2b–c), and cellular morphology (Fig. 2d) at day 4 post transduction. Significant change in c-kit level was only observed for SYNCRIP-depleted cells with one hairpin shRNA (shRNA#2) but not the other shRNA (shRNA#1) (Supplementary Fig. 2d). SYNCRIP-KD also resulted in apoptosis of leukemia cells at 5 days post transduction (Fig 2e and Supplementary Fig. 2e–f), suggesting that differentiating cells subsequently underwent apoptosis. Of note, SYNCRIP function was not restricted to MLL-AF9 driven leukemia; because we observed a similar reduction in colony formation of AML-ETO9a driven leukemia cells depleted for SYNCRIP (Supplementary Fig. 2g–h). We further performed shRNA mediated depletion in MLL-AF9 leukemia cells and found a requirement for leukemia *in vivo*, (Fig. 2f) since diseased mice with SYNCRIP-shRNA expressing leukemia cells selected for attenuated *Syncrip*-knockdown (Supplementary Fig. 2i–j).

To rule out the potential for off-target effects from shRNA mediated knockdown and test an additional leukemia line, we developed *Syncrip*-guide RNAs (gRNAs) for CRISPR/Cas9 mediated deletion. RN2- myeloid leukemia cells (MLL-AF9, NRAS[G12D] and expressing rtTA-RN2 cells[26]) were transduced with vectors expressing the inducible (tetO) Cas9 and gRNAs specific for *Syncrip* or an empty vector (Cas9-EV) and sorted based on GFP positivity after induction by Doxycycline (Dox). We observed reduced colony formation and proliferation with an increase in differentiation (Fig. 2g–i and Supplementary Fig. 2k–l) in SYNCRIP depleted RN2 cells. No significant change in percentage of c-kit high cells was observed upon SYNCRIP depletion (Supplementary Fig. 2m). In mammalian cells there are multiple isoforms of SYNCRIP (UniProtKB - O60506 human SYNCRIP/HNRNP Q). To identify the SYNCRIP isoforms in leukemia, we overexpressed cDNAs encoding 3 different isoforms of SYNCRIP (hnRNP_Q1: 562 amino acids, Q3: 623 amino acids, and Q4: 527 amino acids) in RN2 cells. Immunoblot analysis demonstrated the existence of 2 SYNCRIP isoforms with the dominant isoform being Q1 (562 aa) and the alternative, larger isoform Q3 (623 aa) (Supplementary Fig. 2n). Despite the aggressiveness of the RN2 MLL-AF9 leukemia cells, SYNCRIP overexpression increased colony forming activity, indicating that SYNCRIP overexpression can potentiate leukemic cell growth (Supplementary Fig. 2o). More importantly, overexpression of SYNCRIP dominant isoform (562 aa) in RN2 cells drove a more rapid leukemia in vivo (Fig. 2j).

Consistent with an on-target effect of CRISPR/Cas9 deletion for *Syncrip*, ectopic expression of non-target human *SYNCRIP* could rescue the reduction in colony formation and reverse the increased differentiation from SYNCRIP depletion (Fig. 2k–l and Supplementary Fig. 2p–q). Therefore, our data strongly suggest that SYNCRIP is required for leukemic cell growth, cell survival, and maintenance of the undifferentiated state.

CRIPSR/Cas9 deletion of SYNCRIP differentially impairs leukemogenesis but not normal hematopoiesis

To further assess SYNCRIP function in normal and malignant hematopoiesis *in vivo*, we developed mice deficient for SYNCRIP using CRISPR/Cas9 approach with co-injection of gRNAs and Cas9 mRNA into the pronucleus of mouse zygotes. We then collected fetal liver cells from developed embryos in pseudo moms at E14 and determined fetal liver genotypes by PCR (Fig.3 a–b and Supplementary Fig. 3a and Supplementary table 11). We performed analysis on confirmed wild type (WT) and CRIPSR-knockout samples (CR-KO), and found equivalent frequency of phenotypic HSCs in WTs versus CR-KOs (Fig. 3c and Supplementary Fig. 3b) and a modest increase in colony forming units granulocyte-macrophage (CFU-GM) in the CR-KOs (Supplementary Fig. 3c). We then performed analysis for SYNCRIP functions during normal hematopoiesis *in vivo* by monitoring the engraftment efficiency of WT vs. CR-KO cells in transplanted recipient mice. We confirmed reduction of SYNCRIP protein expression in engrafted bone marrow cells from CR-KO compared to WT recipient (Fig. 3d–e). We observed no defect in engraftment of CR-KO cells in primary transplant mice (Fig. 3f). To determine whether SYNCRIP is required for development of leukemia *in vivo*, we then isolated LSKs cells from bone marrow of *Syncrip* WT and CR-KO primary transplanted mice, transduced them with MLL-AF9-GFP expressing viruses, and injected GFP MLL-AF9 transformed cells into recipient mice (Fig. 3g). We also performed secondary bone marrow transplantation of *Syncrip* WT and CR-KO bone marrow cells into lethally irradiated mice and found a mild reduction in engraftment (Fig. 3h–i). On the other hand, MLL-AF9 transformed LSK cells derived from CR-KO recipients showed a delay in leukemogenesis *in vivo* when compared to WT cells (Fig. 3j). However, we found that expression of SYNCRIP was maintained when the animals died of leukemia (Fig. 3k and Supplementary Fig. 3d). These data imply that the CRISPR-driven KO fetal liver samples were mosaic for both WT and CR-KO *Syncrip*, resulting in the residual SYNCRIP-WT leukemia to grow out. Overall, these data indicate the requirement for SYNCRIP for the development of leukemia in a genetic mouse model.

SYNCRIP is highly expressed and essential for human leukemia cells

To define SYNCRIP's role in human leukemia, we surveyed a previously published expression dataset and found that *SYNCRIP* expression was elevated in AML patients with diverse genetic alterations compared to normal hematopoietic stem and progenitor cells (Fig. 4a)[27]. We also found elevated expression of *SYNCRIP* in other hematological malignancies including T-ALL and B-ALLs with various genetic abnormalities (Supplementary Fig. 4a). High levels of *SYNCRIP* expression were also observed across multiple human myeloid leukemia cell lines compared to normal human CD34 enriched cord blood cells (CB-CD34+ cells)(Supplementary Fig. 4b). We further validated that SYNCRIP was highly expressed at the protein level in human myeloid leukemia cell lines (10/11) and primary patient samples (5 patients) compared to CB-CD34 cells cells (Fig. 4b–c). To test the functional role of the increased SYNCRIP expression in leukemic cells, we transduced myeloid leukemia cells (MOLM13, NOMO-1, KASUMI-1 and NB4) with lentiviral shRNA vectors targeting *SYNCRIP* and obtained efficient knock down of SYNCRIP with 2 independent hairpins. Upon SYNCRIP depletion, we observed reduced cell proliferation and increased apoptosis coupled with increased myeloid differentiation, depending on the particular marker, in the

AML cell lines (Fig. 4d–h and Supplementary Fig. 4c–h). Overall, these data indicates an important role for SYNCRIP in different types of human myeloid leukemia driven by various oncogenic drivers.

SYNCRIP and MSI2 co-regulate leukemia stem cell gene expression programs

To better understand the molecular function of SYNCRIP in leukemia, we performed RNA-sequencing on MLL-AF9 leukemia cells transduced with shRNAs against *Syncrip* four days post-transduction. The transcriptional profile of *Syncrip*-shRNA transduced cells was significantly altered and the results obtained from two independent shRNA hairpins were highly correlated (Supplementary Fig. 5a). We found 282 genes that were differentially expressed, where 57 were downregulated (*Syncrip* was ranked 9th most downregulated gene) and 225 were upregulated (Log_2 Fold change>1.5, FDR<0.01, Supplementary Table 12 and Fig. 5a). We then functionally annotated our RNA-sequencing analysis by performing Gene Set Enrichment Analysis (GSEA)[28] on all curated gene sets in the Molecular Signatures Database (MSigDB, http://www.broadinstitute.org/msigdb; 3,256 gene sets) combined with an additional set of relevant gene sets (92 gene sets from our experimentally derived or published hematopoietic self-renewal and differentiation signatures[28,29]) using the ranked list of differentially expressed genes in *Syncrip*-shRNA samples (Cntrl/*Syncrip*-shRNA; Supplementary Table 13). Genes upregulated after SYNCRIP depletion were enriched in 236 gene sets and downregulated genes were enriched in 172 gene sets (Supplementary Table 14, 15 and 16). Set of genes downregulated in HSCs (CD133+ vs CD133−)[30], LSC related gene signature associated with a good prognosis in AML[31] and the myeloid development program[32] were significantly enriched for upregulated genes in SYNCRIP depleted cells (Fig. 5b–d and Supplementary Table 16). Moreover, we found that MLL-AF9 direct targets were enriched for genes downregulated after SYNCRIP depletion (Fig. 5e–f). In consistent with the MLL program being reversed upon *Syncrip* knockdown, genes negatively regulated by HOXA9/MEIS1 were enriched for genes suppressed by SYNCRIP (Fig. 5g). Overall, these data suggest that SYCNRIP depletion results in a loss of the HSC/LSC program and the MLL-AF9 gene expression program. Based on previous studies[15] and our data, we hypothesized that SYNCRIP and MSI2 may coregulate the LSC/MLL epigenetic program. Consistent with this observation, genes downregulated after SYNCRIP depletion were significantly enriched for MSI2's direct mRNA binding targets (Top HITS-CLIP; Cross-linking immunoprecipitation followed by high throughput RNA-sequencing targets[29]) (Fig. 5h). Furthermore, genes upregulated in SYNCRIP depleted cells were enriched for genes that were also upregulated in *Msi2* deleted LSCs[15] (Fig. 5i). Interestingly, genes regulated by MSI2 including *Hoxa9, c-Myc, Ikzf2*, and *Meis1* were found to be downregulated upon loss of SYNCRIP (Supplementary Fig. 5b).

To evaluate the relevance of these data, we examined a human expression dataset (Fig. 4a) and found that elevated SYNCRIP expression corresponded to an increase in HOXA9/MEIS1 target genes, *IKZF2* and *c-MYC*, but without corresponding to altered MSI2 levels (Supplementary Fig. 5c–g). Taken together, these data suggests that SYNCRIP and MSI2 may coregulate a gene expression program that is essential for myeloid leukemia cells.

*S*YNCRIP and MSI2 interact through shared common mRNA targets

To further probe the interaction between SYNCRIP and MSI2, we performed reciprocal immunoprecipitations in MSI2 overexpressing leukemia cell line (K562) to confirm SYNCRIP as an identified protein-protein interacting partner of MSI2 from our mass-spectrometry data. We detected the interaction by reciprocal immunoprecipitation using antibodies against either MSI2 or SYNCRIP. Interestingly, we found that the interaction is RNA-dependent, as treatment of the lysate with RNAse diminished the interaction between the two proteins (Fig. 6a). Similar interaction was observed in MOLM13, a myeloid leukemia cell line carrying MLL-AF9 fusion protein (Supplementary Fig. 6a), suggesting that SYNCRIP and MSI2 bind to a common set of mRNA targets. To test if SYNCRIP and MSI2 share MSI2's previously validated targets in MLL-AF9 driven leukemia[15], we performed RNA-IP and found that SYNCRIP could also bind *Myc, Hoxa9*, and *Ikzf2* mRNA (Fig. 6b).

SYNCRIP post-transcriptionally regulates HOXA9 expression

Next, we sought to determine whether SYNCRIP regulates expression of these candidate genes. Targeted depletion of SYNCRIP with CRISPR/Cas9 or shRNA hairpins in multiple myeloid leukemia cells (RN2 cells, mouse dsRed MLL-AF9 cells and MOLM13 cells) significantly reduced HOXA9 (Fig. 6c–d and Supplementary Fig 6b–c). A decrease in c-MYC and IKZF2 was observed with CRISPR/Cas9 depletion of SYNCRIP in RN2 cells (Fig. 6c), while reduction in c-MYC was observed at 4 days post transduction compared to 3 days post transduction in both dsRed MLL-AF9 cells and MOLM13 cells (Fig. 6d and Supplementary Fig 6b–c). While these changes occurred at the protein level, we also observed variable reductions in mRNA levels of *HoxA9, c-Myc*, and *Ikzf2* (Supplementary Fig 6d–e, h–j). As previously described, MSI2 depletion reduced HOXA9 and c-MYC protein expression and downregulated *HoxA9, c-Myc*, and *Ikzf2* mRNA levels at 4 days post transduction, similar to the phenotype observed in SYNCRIP knockdown cells (Supplementary Fig 6f–g).

To further understand the mechanism for SYNCRIP regulation of HOXA9 expression, we examined the effects of SYNCRIP depletion on total RNA, but found no change in SYNCRIP depleted cells compared to control cells (Supplementary Fig 6k). Additionally, reduced HOXA9, c-MYC, and IKZF2 protein levels in SYCNRIP depleted cells were not due to an effect on mRNA stability, since mRNA levels of these genes were equivalent after the addition of actinomycin D to block transcription (Supplementary Fig 6l–m). Moreover, measurement of newly synthesized proteins based on AHA incorporation revealed a significant decrease in AHA labeled HOXA9 protein in SYNCRIP depleted cells. Despite its short half-life, c-MYC labeling at day 3 remained unchanged (Fig. 6e), and global peptide synthesis was modestly increased based on quatification of total OP-Puro incorporation (Fig. 6f–g). These data suggest that SYNCRIP in part controls translation of specific targets including HOXA9.

HOXA9 is a functional down stream target of SYNCRIP in leukemia cells

In support of SYNCRIP and MSI2 coregulating the MLL-associated transcriptional program, MSI2 overexpression could rescue the reduced colony formation and reversed the

reduction of HOXA9 after *shRNA-Syncrip* depletion (Fig 7a and Supplementary Fig. 7a–b). Verifying the functional relationship between SYNCRIP and HOXA9, retroviral HOXA9 overexpression partially reversed the reduction in colony formation of dsRed MLL-AF9 cells after SYNCRIP depletion (Fig. 7b–c and Supplementary Fig. 7c–d). Similarly, overexpression of HOXA9 also rescued the cell growth in SYNCRIP-KD MOLM13 cells (Fig. 7d–e). In contrast, forced MYC expression failed to rescue the effects of SYNCRIP depletion (Supplementary Fig.7e–h). Interestingly, MYC protein levels were also reduced after SYNCRIP depletion but remained higher than the controls after shRNA depletion. These data suggest that SYNCRIP maintains translation of the MLL and LSC program in part through its control of HOXA9 expression.

To directly demonstrate the relevance of SYNCRIP function in human leukemia, we knocked down SYNCRIP expression in leukemia cells derived from a primary AML patient (Supplementary table 17) by transducing cells with control shRNA or SYNCRIP-shRNAs. We monitored engraftment of the cells *in vivo* after transplantation of sorted GFP positive transduced cells into recipient mice. Depletion of SYNCRIP protein expression resulted in a marked reduction in engraftment of human CD45 GFP positive leukemia cells at week 10 (for shRNA#1) and week 16 (for both shRNA#1 and #2) (Fig. 7f). Importantly, HOXA9 expression in the primary AML patient cells correlated with extent of SYNCRIP shRNA depletion (Fig. 7g). Altogether, these data demonstrate that SYNCRIP regulates myeloid leukemia cell survival at least in part through regulating expression of HOXA9, a critical target in leukemia.

Discussion

Our study uncovered a functionally dysregulated riboproteomic network in myeloid leukemia by performing an *in vivo* shRNA screen for the MSI2 interactome. We identified several RBPs, including SYNCRIP, which were essential for the survival of myeloid leukemia cells. Other studies have utilized similar approaches to identify novel epigenetic regulators in leukemia e.g. BRD4[33], SIRT-1[34], and *JMJ1c*[19] or to identify unknown functions of cancer associated genes in leukemia e.g. ITGB3[18]. We uncovered an RBP associated network that allowed us to further explore the functional interactions between its components, in particular MSI2 and SYNCRIP. We found that MSI2 and SYNCRIP co-regulated the myeloid leukemia self-renewal post-transcriptional program, including many of the downstream targets of MLL-AF9, specifically HOXA9 (Fig. 7g). RBPs act in concert to orchestrate the regulatory processes of protein expression in the manner similar to many well characterized functional complexes that mediate epigenetic regulation. Thus, we provide a strategy for identifying and functionally characterizing novel RNA binding protein regulators in LSCs.

SYNCRIP regulates expression of genes enriched with MSI2 direct binding mRNAs and binds to mRNA targets of MSI2 including *Hoxa9, Ikzf2*, and *c-Myc*. Mechanistically, we also demonstrated that SYNCRIP regulates synthesis of HOXA9 protein, one of the major functional downstream targets of the MLL-AF9 transcriptional program. These data indicates that SYNCRIP shares with MSI2a set of common target genes, that is critical for leukemia. However, it is likely that SYNCRIP also controls expression of genes that are not

associated with MSI2 or the MLL associated network. Future studies that directly profile SYNCRIP's binding targets would further elucidate our understanding of SYNCRIP's function in leukemia.

SYNCRIP's function in normal development and in cancer is poorly characterized. It has been mostly studied in the context of neuronal tissue and mRNA trafficking in neurons[20,24,25]. Only recently has SYNCRIP been implicated in exosomal miRNA sorting in hepatocyte cells[35]. Using both loss and gain of function approaches *in vitro* and *in vivo*, we demonstrated a requirement for SYNCRIP as a novel cooperating oncogene in myeloid leukemia. We also created a rapid SYNCRIP knockout (KO) with CRIPSR/Cas9 by taking advantage of the unique ability of hematopoietic stem cells to engraft and reconstitute the recipient's blood system. This system demonstrated that SYNCRIP is differentially required in leukemia cells compared to normal cells. Nevertheless it will be important to further study SYNCRIP's role in hematopoiesis.

In human AML, SYNCRIP expression was elevated in AML cell lines and in patients compared to normal cells. This supports the differential requirements for SYNCRIP in leukemia cells vs. normal cells, suggesting that SYNCRIP is a potential therapeutic target in AML. Interestingly, dysregulation of MSI2 in AML was previously described as a predictor of poor survival in MDS[36] and AML[12], and future studies will determine if SYNCRIP can similarly be a useful diagnostic marker in leukemia.

In summary, as the roles for RBPs in leukemia and cancer have become clinically relevant, they represent a new class of targets for therapeutic interventions. Small molecule inhibitors that specifically block RBPs binding to RNAs or antisense oligionucleotides (ASOs) and can knockdown these proteins could provide a strategy for targeting these RBP complexes[37–40]. Overall, we propose that targeting the riboproteomic network in leukemia could be a novel therapeutic strategy in cancer.

Online methods

Mass Spectrometry Methods and Analysis (used for Pool 3)

K562 cells were grown with either MSCV-IRES-GFP or with FLAG-MSI2 and immunoprecipitated with FLAG antibody as previously described[15]. 150 million cells per experiment were then stained, and the gel was cut into eight slices by the Children's Proteomics Core Facility. Control and MSI2 interacting proteins were considered to be represented if there were two or more peptides found and there was high confidence with a MASCOT score of either equal or greater than 20 or 77. Pairwise analysis was performed for two independent immunoprecipitation experiments and mass spectrometry analyses. TOPGENE was performed with 234 MSI2 direct binding targets.

Intestinal MSI-1 CLIP-CHIP used for pool 2 gene prioritization

UV-crosslinked mouse intestine was immunoprecipitated for MSI1. Similar CLIP protocol was performed as in Park et al. 2014[29], with the exception that RNA was random primed and hybridized to Affymetric arrays 1.0ST array. Fold enrichment was ranked over IgG.

Pool description for gene prioritization used for the in vivo shRNA screen

The number of genes used in our screen was determined based on our previous studies that included approximately 100 genes[22]. Therefore, the genes in each pool were prioritized based on the following criteria. Pool 1 is made up of two sub-pools, 1a and 1b. Pool 1a was composed of differentially expressed genes prioritized based on our Msi2 gene expression and other hematopoietic gene sets with a matrix score of 6 or more (Supplementary Table 3). Pool 1b was selected based on genes found in the leading edge taken from the GSEA with MSI2 overexpression in LSK cells overlapped with genes upregulated after shRNA depletion in CML/AML cell lines or leading edge genes in the rank list of Msi2 KO LSKs. Genes previously determined canonical targets Numb, Numbl and CDKN1A, were added (Supplementary Table 4).

Pool 2 genes were chosen based on an intestinal CLIP-CHIP (UV-crosslinked mouse intestine) and immunoprecipitation for MSI1. MSI1 bound targets were ranked for the top 1000 genes, binding of the 3′UTR and their fold enrichment over the IgG control (Supplementary Table 5). These genes were ranked if they were MSI2-hematopoietic relevant genes. A combined score of 3 or more were included into the screen (Supplementary Table 6).

Pool 3 included MSI2 direct protein-protein interactors. A matrix score of 3 or more were chosen based on their ability to interact with MSI2 and was included in a MSI2 or hematopoietic relevant gene set (Supplementary Table 7). A summarized list of genes included in the shRNA screen is listed in (Supplementary Table 8).

Lentiviral production, infection, and *in vivo* shRNA screen

Lentiviruses expressing shRNAs in the pLKO.1 vectors were obtained from RNAi consortium at the Broad Institute. Virus production and preparation of pooled and titered lentiviruses for screening was performed as previously described[18]. Pooled titered virus was thawed and kept on ice. L-GMPs (c-kit high cells top 50% were sorted). Infection, 12 well dishes were resuspended into 600uL virus + 600uL of cells ($2*10^6$ cells) per replicate 1.2mL/well. Cells were spinfected (2500RPM 90 minutes) and then cells were split for day 0 sequencing or injected into sublethally irradiated mice. Five pools representing a random set if ~100 shRNAs per pool with a total of titered 627 shRNA viruses were generated and used to transduce leukemia cells. Each transducing well was split: half was kept for sequencing and half was transplanted (1 million cells) into a sublethally irradiated recipient mice. There were five replicates per pool with five mice per pool with an experiment representing 25 total mice. After two weeks, cells were harvested from bone marrow and spleen and previously frozen cells for sequencing analysis.

Isolation and infection and selection of murine leukemia and normal cells

Tibia and femurs, pelvis, and arm bones from leukemia or C57Bl/6 wild type mice (6–8 week old) were harvested, crushed, filtered, and subjected to red blood cell lysis (Qiagen). To isolate c-kit positive cells, bone marrow cells were incubated with CD117 microbeads (Miltenyi Biotec), according to manufacturer's instructions, and then subjected to positive selection using autoMACS Pro Separator. Cells were spinfected in RPMI with 10% FBS and

cytokines: SCF (10 ng/ml), IL-3 (10 ng/ml), and IL-6 (10 ng/ml) and GM-CSF (10 ng/ml). 48 hours post-transduction, cells were treated with 2 μg/ml puromycin. Two days after puromycin selection, cells were harvested for further analysis.

Colony forming assay

10,000 cells were plated on methocult GFM3434 (Stemcell Technologies). Colonies were scored every five days for leukemia cells and every seven days for normal ckit-enriched bone marrow cells.

In vivo transplantation of leukemia cells

MLL-AF9 tertiary mouse leukemia cells were transduced with lentiviruses expressing puromycin and shRNAs against *Syncrip* or a control shRNA. Transduced cells were selected by 2 μg/ml puromycin for 2 days. 50,000 selected cells were injected retro-orbitally into female C57Bl/6 (6–8 week old) recipient mice that had been sublethally irradiated with 475 cGy. All animal studies were performed on animal protocols approved by the Institutional Animal Care and Use Committee (IACUC) at Memorial Sloan Kettering Cancer Center.

CRISPR/Cas9 approach to create *Syncrip*-CRISPR-knock out (CR-KO)

The CRISPR gRNAs used for deleting exon 3 and 4 of the *Syncrip* gene were designed using the approach of Romanienko et. al[41]. The sequence for the 5′-gRNA is GTACCTGTATTACCCAATGC and sequence for the 3′-gRNA is CAATTTGGAATTGACCGCAC. Both were produced by *in vitro* transcription using the pU6T7 promoter in the hybrid plasmid described. To initiate cleavage of the target locus in mice, gRNA (C67) and gRNA (C69) in conjunction with Cas9 mRNA were co-injected into the pronucleus of mouse zygotes at a concentration of 50 ng/ul each, using conventional techniques (Manipulating the Mouse Embryo: A Laboratory Manual). Deleted samples were assayed using PCR primers located outside of the gRNA cleavage sites (outside *Syncrip* exon 3–4) thereby revealing the size of the deletion based on the nucleotide length of the amplicon obtained (~ 900bp for WT vs. ~ 300 bp for deletion).

Isolation of fetal liver cells, PCR genotyping and bone marrow transplantation

Fetal liver cells were isolated and single cell suspended based on standard protocols[42]. ~ 200,000 fetal liver cells after red blood cell lysis were used for DNA extracting using HotSHOT genomic DNA preparation methods. 2 ul supernatant containing DNA was used for PCR reactions with specific primers for detection of *Syncrip* exon 3–4. DNA was resolved in agarose gel 1.5%. 500,000 cells from confirmed WT and Syncrip-CR-KO fetal livers were retro-orbitally injected into lethally irradiated CD45.1 recipient mice. For secondary transplantation, 1 million bone marrow cells were retro-orbitally injected into lethally irradiated CD45.1 recipient mice.

Generation of MLL-AF9 primary leukemia and transplantation

Bone marrow cells from 6- to 10-week-old transplanted $WT^{fl/fl}$ or *CR-SYNCRIP KO* / mice were isolated and subsequently enriched for c-kit positive cells. c-kit enriched cells were stained with Lineage antibody cocktail (CD3, CD4, CD8, Gr1, B220, CD19,

TER119 conjugated with PeCy5), Sca-Pac Blue, CD34-FITC, SLAM-APC, CD48-PE, and c-KIT-APC-Cy7. Lin-Sca$^+$Kit$^+$ cells were sorted using a BD FACS Aria. Sorted cells were grown overnight in SFEM medium with 10 ng/ml IL-3, 10 ng/ml IL-6, 50 ng/ml SCF, 10 ng/ml thrombopoietin (TPO), and 20 ng/ml FLT3L. Cells were transduced twice with supernant containing retroviruses expressing MLL-AF9 and GFP (a gift from Scott Armstrong, Memorial Sloan Kettering Cancer Center) on retronectin-coated 96 well flat-bottom plates. The cells were expanded for one week in GFM3434 methylcellulose (Stem Cell Technologies). MLL-AF9 transformed cells were sorted base on GFP positivity. 200,000 GFP sorted$^+$ cells and 250,000 helper cells were injected retro-orbitally into each lethally irradiated 6–8 week-old C57BL/6 mouse.

Proliferation assay of human leukemia cells

Human leukemia cells were infected with viruses expressing scramble and hairpins against SYNCRIP by spinfection of cells in RPMI with 10% FBS together with viral supernatant. After 48 hours of infection, cells were treated with 3 μg/ml puromycin. Two days after puromycin selection, cells were plated at 250,000 cells/ml for proliferation assay. Cells were counted everyday using MUSE cell analyzer (Millipore) after plating. Cell growth was calculated based on normalization of cell number to cell number at plating. All cell lines were purchased from ATCC, authenticated by Genetica and tested negative for mycoplasma contamination.

Intracellular staining and flow cytometry

For intracellular staining, cells were fixed with 1.5% paraformaldehyde at room temperature for 15 minutes and permeabilized with ice-cold methanol. Cells were washed 3 times with PBS and incubated with SYNCRIP antibody (MAB11004, Milipore) in 2% FBS PBS for 1 hour at room temperature. Cells were then washed twice with PBS and incubated with secondary antibody conjugated with Alexa Fluor 647 (Molecular Probes) for 30 min at room temperature. Cells were washed with PBS and resuspended prior to analysis using BD Fortessa instrument.

Cells were stained for Mac1-PB, Gr1-APC, F480-PE-Cy7, CD115-APC and c-Kit-APC-Cy7 and analyzed on a BD FACS LSR Fortessa instrument to assess differentiation status of wild type and knockdown leukemia cells. For stem and progenitor cells analysis of fetal liver hematopoietic cells, 10^6 cells were stained with stem/progenitor cells' antibody panel including: lineage antibody cocktail (CD3, CD4, CD8, Gr1, B220, CD19, TER119 conjugated with PeCy5), Sca-Pac Blue, KIT-APC-Cy7, CD34-FITC, CD16/32-PE-CY7, CD48-PE and SLAM-CD150-APC. For analysis of engraftment in recipient mice, 10^6 bone marrow cells were stained with stem/progenitor cells' antibody panel and CD45.1-PE-Texas Red and CD45.2-A700.

To measure apoptosis, cells were washed with PBS and incubated with anti–ANNEXIN-V-PE (BD Biosciences) in the ANNEXIN-V binding buffer (10 mM HEPES, pH 7.4, 140 mM NaCl, 4 mM KCl, 0.75 mM MgCl$_2$, 1 mM CaCl$_2$) in a reaction volume of 100 μl for 15 minutes. DAPI was added prior to analysis using a BD Fortessa instrument.

O-Propargyl-puromycin (OP-puro) flow analysis

Cells were plated at 100,000 cells/ml density and treated with 50 uM OP-Puro (NU-931-05, Jena Bioscience). Control cells were treated with cyclohexamide (CHX) at 150 ug/ml for 15 minute. Cells were washed twice prior to collection and subjected to processed using Click-iT® Flow Cytometry Assay Kit (C10418 – Invitrogene) following the manufacturer's instructions. Labelled cells were analyzed using BD Fortessa instrument.

Immunoprecipitation and immunoblot analysis

K562 cells were collected by spinning down at 1,500 rpm for five minutes at 4°C, washed twice with PBS, and then resuspended thoroughly at 2×10^7 per ml in 1X Ripa buffer (BP-115- Boston BioProducts) with freshly added DTT (1mM) and proteinase inhibitor cocktail. The cells were incubated for 30 min on ice. Supernatant was then collected after the mix was spun at 14,000 rpm for 30 min at 4°C. For each immunoprecipitation assay, 250 ul of cell extract was mixed with 750 ul of 1X Ripa buffer 2 ug of anti-mouse/anti-SYNCRIP antibody or 2 ug anti-rabbit/anti-MSI2 and 50 ul agarose beads. For RNA independent assay, lysates were treated with RNase A (1ug/ml) for 30 min at 37°C prior to coimmunoprecipitation reactions. After rotating at 4°C overnight, beads were washed 5 times with 1X Ripa buffer and boiled with 1X Lamine protein running buffer.

For immunoblot analysis, cells were counted and washed twice with cold PBS prior to collection. ~ 250,000 were resuspended and lysed in 40 ul 1X Lamine protein running buffer and boild for 5 minutes. Whole cell lysates were run on 4%–15% gradient SDS-PAGE and transferred to nitrocellulose membrane. Membranes were blotted for SYNCRIP (MAB11004 or 05-1517-Milipore), IKZF2 (sc-9864; Santa Cruz), HOXA9 (07–178; Millipore and ab140631, Abcam), MYC (5605S; Cell Signaling), MSI2 (ab76148; Abcam), and ACTIN (A3854; Sigma-Aldrich).

RNA immunoprecipitation

30×10^6 RN2 leukemia cells were used for RNA-IP using the Magna RIP RNA-binding protein immunoprecipitation kit (03–115; Millipore). First, cells were washed with cold PBS and then lysed. Anti-rabbit antibody or anti-MSI2 antibody (Millipore); anti-mouse or anti-SYNCRIP (18E4 Millipore) incubated with magnetic beads was used to immunoprecipitate MSI2 and SYNCRIP. After washing of the immunoprecipitated complexes, they were treated with proteinase K. RNA extraction was performed by the phenol/chloroform method, and purified RNA was converted to cDNA using the Verso cDNA kit (Thermo Scientific). Quantitative PCR was used for validating target mRNAs bound by MSI2 and SYNCRIP.

mRNA stability analysis

Control and SYNCRIP depleted cells were treated with 5ug/ml of Actinomycin D and harvested at indicated time points. Total RNA was isolated using RNeasy RNA extraction kit. 200 ng of RNA was used for reverse transcription reaction and quantitative RT-PCR for *Syncrip, Hoxa9, Ikzf2, Myc* and *β-actin* was performed. *β-actin* served as house keeping gene control. Relative mRNA levels are normalized to the starting point of treatment.

Metabolic labeling and capture of newly synthesized protein

Newly synthesized proteins were labeled using the Click-iT Protein Labeling Kit (Invitrogen). For this, 48 hours after infection with corresponding shRNA-expressing plasmids, 1×10^7 MOLM13 selected cells were cultured at 1×10^6 cells/mL in fresh media for 14 hours. After one wash with PBS, cells were resuspended in methionine-free RPMI 1640 medium (Gibco) supplemented with 10% dialyzed FBS (Gibco) for 30 min, at which point the methionine analog L-azidohomoalanine (AHA) was added (50 μM, 14 hours) to allow incorporation of AHA into nascent proteins. Cells were harvested and lysed in 50 mM Tris-HCl, pH 8.0, 1% SDS, with protease and phosphatase inhibitor mixes (cOmplete and PhosSTOP, Roche). 150 μg of total protein (up to 50 μL of lysate) were used in the crosslinking of AHA-labeled nascent proteins to an alkyne-derivatized biotin in the Click-iT Protein Reaction Buffer (Invitrogen) according to manufacturer's instructions. The resulting precipitated total protein pellet was resolubilized in 100 μL of 1% SDS PBS with protease inhibitors by pipetting, vortexing and incubating at 70°C for 10 minutes. The SDS was then quenched with 100 μL of 6% NP-40 in PBS with protease inhibitors. After centrifuging at 15,000 g for 5 minutes at room temperature for removing any insoluble particles, biotin-crosslinked nascent proteins were then captured overnight with streptavidin-coated Dynabeads M-280 (Invitrogen) and then eluted from the beads by boiling the samples for 5 min in 2% SDS loading buffer for Western Blot. Previously, beads were thoroughly washed with PBS with 0.1% bovine serum albumin and 2% NP-40, first, and finally with PBS. The whole volume of AHA-labeled, biotin-crosslinked, streptavidin-pulled down protein was separated by SDS-PAGE together with lysate depleted of nascent protein after streptavidin incubation and input lysates.

RNA purification and quantitative RT-PCR

RNA extraction for quantitative Real time PCR (qRT-PCR) and RNA-sequencing Total RNA was isolated using TRIzol and the Qiagen RNeasy Plus® mini kit (QIAGEN, Germany). cDNA was generated from RNA using iScript™ cDNA Synthesis (Biorad Kit #1708891) with random hexamers according to the manufacturer's instructions. Real-time PCR reactions were performed using an ABI 7500 sequence detection system. Quantitative PCR for actin was performed to normalize for cDNA loading. Relative quantification of the genes was calculated using the method ($2^{\wedge}$-Ct) as described by the manufacturer.

RNA sequencing

Total RNA was isolated from 9 individually transduced and processed MLL-AF9 murine leukemia cells (n=3 for each group including shRNA against luciferase, two shRNAs against SYNCRIP) using TRIzol and the Qiagen RNeasy Plus® mini kit (QIAGEN, Germany). RNA was denatured and 1st chain of cDNA was synthesized using oligo-dT primer containing illumina-compatible linker sequence. After removal of RNA 2nd cDNA chain was synthesized with random decamer containing another illumina-compatible linker sequence. Illumina compatible annealing sequences and external barcodes were introduced during amplification of the libraries.

Differential expression and pathway analysis

Quality Control of raw reads was done using FastQC (v0.11.2) to make sure there were no major flaws in sequencing. They were then mapped to mm10 genome using STAR (v2.3.0e_r291) and default parameters. The mapped reads were counted using htseq-count (v0.6.0, parameters –t exon) and gene models from Ensembl (Mus_musculus.GRCm38.75.gtf). Differential expression was performed using DESeq2 (v1.2.10, default parameters).

Statistical analysis

Student's *t* test was used for significance testing in the bar graphs, except where stated otherwise. A two-sample equal variance with normal distribution was used. The investigators were not blinded to the sample groups for all experiments. *P* values less than 0.05 were considered significant. Graphs and error bars reflect mean + s.e.m, except where stated otherwise.

For animal study, survival probabilities were estimated using the Kaplan-Meier method and compared with the log-rank test. Ten mice per group were chosen to have an estimated 80% power in detecting a greater than 1.50 s.d difference in means at a significance level of $\alpha = 0.05$ using a two-sided test. All animals were randomly assigned to the experimental groups.

All statistical analyses were carried out using GraphPad Prism 4.0 and the R statistical environment.

Supplementary Material

Refer to Web version on PubMed Central for supplementary material.

Acknowledgments

References

1. Lindsley RC, Ebert BL. The biology and clinical impact of genetic lesions in myeloid malignancies. Blood. 2013; 122:3741–8. [PubMed: 23954890]

2. Maynadie M, et al. Twenty-five years of epidemiological recording on myeloid malignancies: data from the specialized registry of hematologic malignancies of Cote d'Or (Burgundy, France). Haematologica. 2011; 96:55–61. [PubMed: 20971817]

3. Bonnet D, Dick JE. Human acute myeloid leukemia is organized as a hierarchy that originates from a primitive hematopoietic cell. Nat Med. 1997; 3:730–7. [PubMed: 9212098]

4. Hope KJ, Jin L, Dick JE. Acute myeloid leukemia originates from a hierarchy of leukemic stem cell classes that differ in self-renewal capacity. Nat Immunol. 2004; 5:738–43. [PubMed: 15170211]

5. Lukong KE, Chang KW, Khandjian EW, Richard S. RNA-binding proteins in human genetic disease. Trends Genet. 2008; 24:416–25. [PubMed: 18597886]

6. Wurth L. Versatility of RNA-Binding Proteins in Cancer. Comp Funct Genomics. 2012; 2012:178525. [PubMed: 22666083]

7. Narla A, Ebert BL. Translational medicine: ribosomopathies. Blood. 2011; 118:4300–1. [PubMed: 22021450]

8. Calado RT, et al. Constitutional hypomorphic telomerase mutations in patients with acute myeloid leukemia. Proc Natl Acad Sci U S A. 2009; 106:1187–92. [PubMed: 19147845]

9. Devlin EE, Dacosta L, Mohandas N, Elliott G, Bodine DM. A transgenic mouse model demonstrates a dominant negative effect of a point mutation in the RPS19 gene associated with Diamond-Blackfan anemia. Blood. 2010; 116:2826–35. [PubMed: 20606162]

10. Cancer Genome Atlas Research N. Genomic and epigenomic landscapes of adult de novo acute myeloid leukemia. N Engl J Med. 2013; 368:2059–74. [PubMed: 23634996]

11. Dvinge H, Kim E, Abdel-Wahab O, Bradley RK. RNA splicing factors as oncoproteins and tumour suppressors. Nat Rev Cancer. 2016; 16:413–30. [PubMed: 27282250]

12. Kharas MG, et al. Musashi-2 regulates normal hematopoiesis and promotes aggressive myeloid leukemia. Nat Med. 2010; 16:903–8. [PubMed: 20616797]

13. Ito T, et al. Regulation of myeloid leukaemia by the cell-fate determinant Musashi. Nature. 2010; 466:765–8. [PubMed: 20639863]

14. Byers RJ, Currie T, Tholouli E, Rodig SJ, Kutok JL. MSI2 protein expression predicts unfavorable outcome in acute myeloid leukemia. Blood. 2011; 118:2857–67. [PubMed: 21753187]

15. Park SM, et al. Musashi2 sustains the mixed-lineage leukemia-driven stem cell regulatory program. J Clin Invest. 2015; 125:1286–98. [PubMed: 25664853]

16. Kwon HY, et al. Tetraspanin 3 Is Required for the Development and Propagation of Acute Myelogenous Leukemia. Cell Stem Cell. 2015; 17:152–64. [PubMed: 26212080]

17. Krivtsov AV, Armstrong SA. MLL translocations, histone modifications and leukaemia stem-cell development. Nat Rev Cancer. 2007; 7:823–33. [PubMed: 17957188]

18. Miller PG, et al. In Vivo RNAi screening identifies a leukemia-specific dependence on integrin beta 3 signaling. Cancer Cell. 2013; 24:45–58. [PubMed: 23770013]

19. Zhu N, et al. MLL-AF9- and HOXA9-mediated acute myeloid leukemia stem cell self-renewal requires JMJD1C. J Clin Invest. 2016; 126:997–1011. [PubMed: 26878175]

20. Mizutani A, Fukuda M, Ibata K, Shiraishi Y, Mikoshiba K. SYNCRIP, a cytoplasmic counterpart of heterogeneous nuclear ribonucleoprotein R, interacts with ubiquitous synaptotagmin isoforms. J Biol Chem. 2000; 275:9823–31. [PubMed: 10734137]

21. Grosset C, et al. A mechanism for translationally coupled mRNA turnover: interaction between the poly(A) tail and a c-fos RNA coding determinant via a protein complex. Cell. 2000; 103:29–40. [PubMed: 11051545]

22. Cho S, et al. BiP internal ribosomal entry site activity is controlled by heat-induced interaction of NSAP1. Mol Cell Biol. 2007; 27:368–83. [PubMed: 17074807]

23. Weidensdorfer D, et al. Control of c-myc mRNA stability by IGF2BP1-associated cytoplasmic RNPs. RNA. 2009; 15:104–15. [PubMed: 19029303]

24. Chen HH, et al. hnRNP Q regulates Cdc42-mediated neuronal morphogenesis. Mol Cell Biol. 2012; 32:2224–38. [PubMed: 22493061]

25. Xing L, Yao X, Williams KR, Bassell GJ. Negative regulation of RhoA translation and signaling by hnRNP-Q1 affects cellular morphogenesis. Mol Biol Cell. 2012; 23:1500–9. [PubMed: 22357624]

26. Zuber J, et al. Toolkit for evaluating genes required for proliferation and survival using tetracycline-regulated RNAi. Nat Biotechnol. 2011; 29:79–83. [PubMed: 21131983]

27. Bagger FO, et al. HemaExplorer: a database of mRNA expression profiles in normal and malignant haematopoiesis. Nucleic Acids Res. 2013; 41:D1034–9. [PubMed: 23143109]

28. Subramanian A, et al. Gene set enrichment analysis: a knowledge-based approach for interpreting genome-wide expression profiles. Proc Natl Acad Sci U S A. 2005; 102:15545–50. [PubMed: 16199517]

29. Park SM, et al. Musashi-2 controls cell fate, lineage bias, and TGF-beta signaling in HSCs. J Exp Med. 2014; 211:71–87. [PubMed: 24395885]

30. Jaatinen T, et al. Global gene expression profile of human cord blood-derived CD133+ cells. Stem Cells. 2006; 24:631–41. [PubMed: 16210406]

31. Yagi T, et al. Identification of a gene expression signature associated with pediatric AML prognosis. Blood. 2003; 102:1849–56. [PubMed: 12738660]

32. Brown AL, et al. Genetic regulators of myelopoiesis and leukemic signaling identified by gene profiling and linear modeling. J Leukoc Biol. 2006; 80:433–47. [PubMed: 16769770]

33. Zuber J, et al. RNAi screen identifies Brd4 as a therapeutic target in acute myeloid leukaemia. Nature. 2011; 478:524–8. [PubMed: 21814200]

34. Chen CW, et al. DOT1L inhibits SIRT1-mediated epigenetic silencing to maintain leukemic gene expression in MLL-rearranged leukemia. Nat Med. 2015; 21:335–43. [PubMed: 25822366]

35. Santangelo L, et al. The RNA-Binding Protein SYNCRIP Is a Component of the Hepatocyte Exosomal Machinery Controlling MicroRNA Sorting. Cell Rep. 2016; 17:799–808. [PubMed: 27732855]

36. Taggart J, et al. MSI2 is required for maintaining activated myelodysplastic syndrome stem cells. Nat Commun. 2016; 7:10739. [PubMed: 26898884]

37. Minuesa G, et al. A 1536-Well Fluorescence Polarization Assay to Screen for Modulators of the MUSASHI Family of RNA-Binding Proteins. Comb Chem High Throughput Screen. 2014; 17:596–609. [PubMed: 24912481]

38. Fox RG, et al. Image-based detection and targeting of therapy resistance in pancreatic adenocarcinoma. Nature. 2016; 534:407–11. [PubMed: 27281208]

39. Zearfoss NR, et al. A conserved three-nucleotide core motif defines Musashi RNA binding specificity. J Biol Chem. 2014; 289:35530–41. [PubMed: 25368328]

40. Lan L, et al. Natural product (−)-gossypol inhibits colon cancer cell growth by targeting RNA-binding protein Musashi-1. Mol Oncol. 2015; 9:1406–20. [PubMed: 25933687]

41. Romanienko PJ, et al. A Vector with a Single Promoter for In Vitro Transcription and Mammalian Cell Expression of CRISPR gRNAs. PLoS One. 2016; 11:e0148362. [PubMed: 26849369]

42. Hemann M. Reconstitution of Mice with Modified Hematopoietic Stem Cells. Cold Spring Harb Protoc. 2015; 2015:679–84. [PubMed: 26134903]
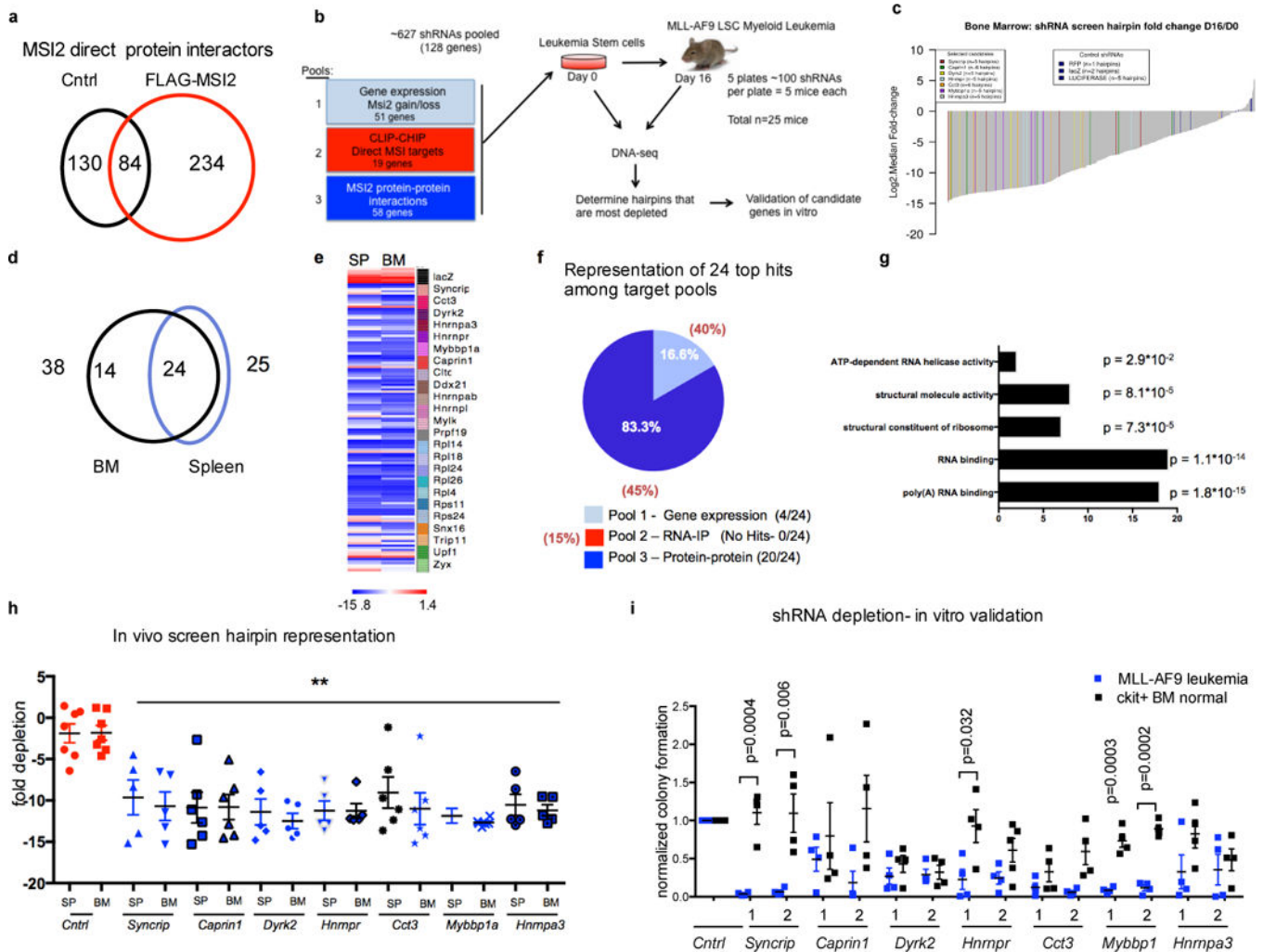
Fig.1. Mass spectrometry of the MSI2 riboproteome and in vivo shRNA screen uncovers the functionally dysregulated RBP network in leukemia

(**a**) Venn diagram showing mass spectrometry analysis of Flag-MSI2 immunoprecipitation in K562 cells transduced with FLAG-MSI2 or empty vector (**b**) Summary of the pooled shRNA screening strategy from primary leukemia cells. (**c**) Waterfall plot depicting normalized depletion levels of all shRNAs in bone marrow (BM). Control shRNAs and hairpins targeting selected candidate genes were highlighted. (**d**) Venn diagram showing score of 24 hits in bone marrow and spleen samples (**e**) Heatmap depicting normalized depletion levels of all shRNAs targeting top 24 genes scored both in bone marrow (BM) and spleen (SP). (**f**) Pie chart showing the scoring percentage of each screening pool in comparison to the predicted score based on pool representation (**g**) GO analysis of top 24 genes scored in in vivo screen (**h**) Log$_2$fold depletion in the bone marrow (BM) and spleen (SP) of all the shRNAs against seven candidate genes in the pooled shRNA screen. error bars, s.e.m **p < 0.01 two tailed *t* test. (**i**) Colony formation was impaired in KD leukemia cells. Number of formed colonies was normalized to that of control MLL-AF9 leukemia cells or control normal c-kit enriched bone marrow cells. n=4 independent experiments; error bars, s.e.m. P value calculated by two tailed *t* test.
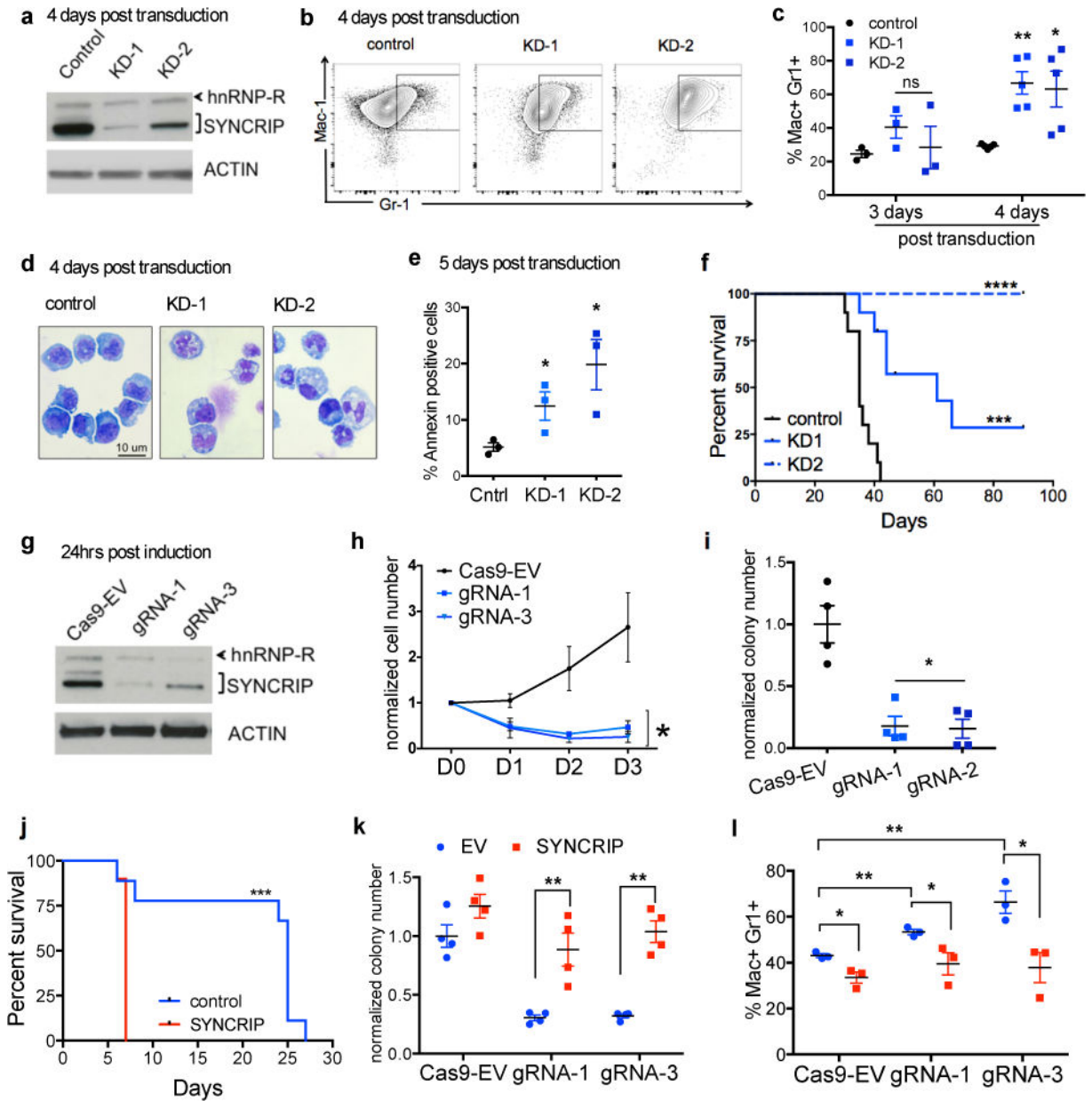
Fig.2. SYNCRIP is required to maintain myeloid leukemia survival in vitro and in vivo
(**a**) Efficient knockdown of SYNCRIP in mouse MLL-AF9 leukemia cells. (**b**) shRNA
depletion of SYNCRIP promoted myeloid differentiation of leukemia cells. Representative
FACS plot of control and SYNCRIP-KD leukemia cells. (**c**) Quantitative summary of FACS
analysis of Gr-1 and Mac-1 expression in control and SYNCRIP-KD leukemia cells 3 days
and 4 days post transduction, n=3 and n=5, respectively, independent experiments; error
bars, s.e.m. ** p<0.01, * p<0.05 two tailed *t* test. (**d**) Giemsa staining of control and
SYNCRIP-KD leukemia cells 4 days post transduction. Original magnification 63X, 1.4 NA
Scale bars: 10 uM. (**e**) Annexin-V assessed by flow cytometry 5 days post transduction. n=3
independent experiments; error bars, s.e.m. ** p<0.01, * p<0.05 two tailed *t* test. (**f**) Kaplan
Meier analysis of leukemia-free survival after injection of SYNCRIP depleted or control

cells into sub-lethally irradiated mice. n=10 for each group, Mantel-Cox test *** p<0.001, **** p<0.0001. (**g**) Reduction of SYNCRIP expression in MLL-AF9 leukemia cells with mutant NRAS expressing a rtTA (RN2 cells) and transduced with tet(O)-inducible Cas9-GFP expressing guide RNAs specific for *Syncrip* (gRNA1 and gRNA3) or Cas9-GFP empty gRNA (Cas9-EV). (**h**) Cells from **g** plated and counted for cellular growth control (black) and two gRNAs (blue). n=3 independent experiments; error bars, s.e.m. * p<0.05 two tailed *t* test (**i**) Cells from **g** were plated into methylcellulose colony assay. n=4 independent experiments; error bars, s.e.m. * p<0.05 two tailed *t* test (**j**) Kaplan Meier analysis of leukemia-free survival after injection of RN2 cells overexpressing SYNCRIP or carrying control- empty vector into sub-lethally irradiated mice n=10 for each group, Mantel-Cox test *** p<0.001 (**k**) Overexpression of SYNCRIP rescued colony forming ability of RN2 cells depleted of endogenous SYNCRIP. n=4 independent experiments; error bars, s.e.m. ** p<0.01 two tailed *t* test. (**l**) Quantitative summary of FACS analysis of Gr-1 and Mac-1 expression in Cas9-EV and *Syncrip*-gRNAs transduced leukemia cells in **k**. n=3 independent experiments; error bars, s.e.m. *p<0.05, ** p<0.01 two tailed *t* test.
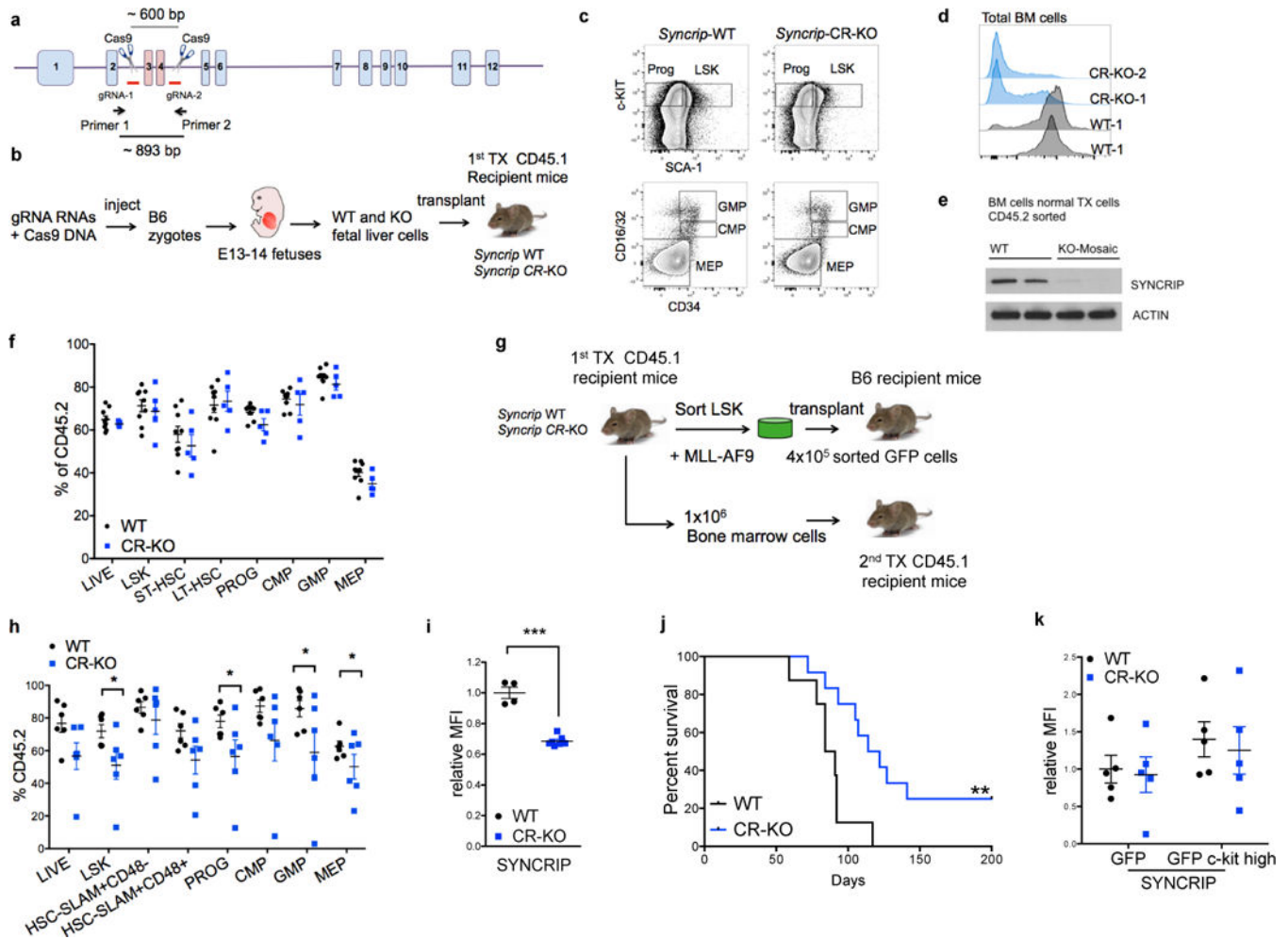
Fig.3. SYNCRIP is required for leukemogenesis in vivo

(**a**). Diagram depicts *Syncrip* locus and CRISPR/Cas9 targeting strategy for generation of *Syncrip*-CR-knockout (KO) and (**b**) experimental scheme for generation of hematopoietic *Syncrip*-CR-KO using CRISPR/Cas9 approach and bone marrow transplantation of fetal liver cells. (**c**) Representative FACS analysis of hematopoietic stem and progenitor cells in WT and *Syncrip*-CR-KO fetal livers. (**d**) Representative FACS histograms of SYNCRIP intracellular staining and (**e**) immunblot analysis of CD45.2 positive bone marrow cells isolated from WT and *Syncrip*-CR-KO recipient mice. (**f**) Quantitative summary of FACS analysis of hematopoietic stem and progenitor compartments in WT and *Syncrip*-CR-KO recipient mice. LIVE: total bone marrow cells; LSK: Lin-Sca1+Kit- cells; PROG: Progenitor cells; GMP: Granulocyte Macrophage progenitor; CMP: Common Myeloid progenitor; MEP: Megakaryocyte-Erythrocyte progenitor. WT n=9; CR-KO n=5. (**g**) Experimental scheme for LSK-derived MLL-AF9 initiation leukemia transplantation model and secondary bone marrow transplantation. (**h**) Quantitative summary of FACS analysis of hematopoietic stem and progenitor compartments in WT and *Syncrip*-CR-KO secondary recipient mice. WT n=6; CR-KO n=6, error bars, s.e.m. *p<0.05 two tailed *t* test. (**i**) Quantitative summary of relative median fluorescence intensity (MFI) analysis of SYNCRIP intracellular staining of engrafted CD45.2 cells in WT and *Syncrip*-CR-KO secondary recipient mice. WT n=4;

CR-KO n=7 error bars, s.e.m. ***p<0.001 two tailed *t* test. (**j**) Kaplan Meier analysis of leukemia free survival after injection of MLL-AF9 transformed WT and *Syncrip*-CR-KO cells into lethally irradiated mice WT n=8, *Syncrip*-CR-KO n=12; Mantel-Cox test ** p<0.01. (**k**) Quantitative summary of relative MFI analysis of SYNCRIP intracellular staining of GFP positive and GFP positive c-kit high cells from mice succumbed to leukemia in WT vs. *Syncrip*-CR-KO. WT n=5; CR-KO n=5.
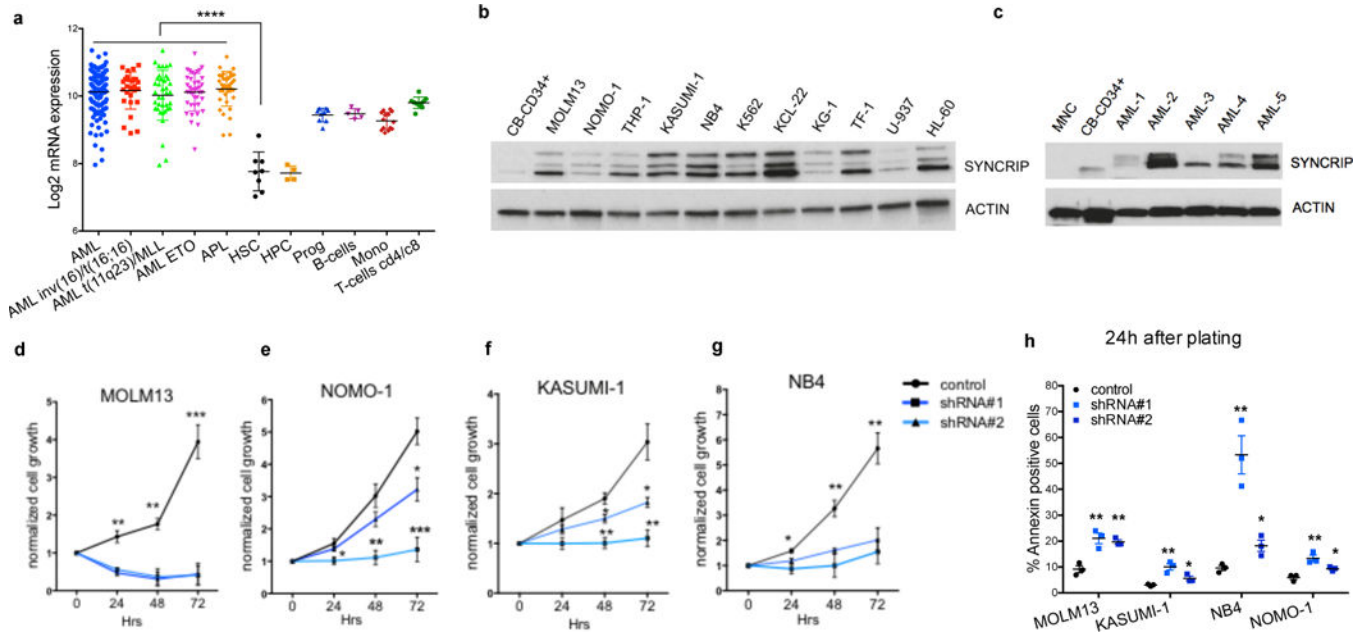
Fig. 4.

***SYNCRIP* is highly expressed in human AML cell lines and primary patient samples, and SYNCRIP depletion results in inhibition of cell growth and apoptosis in human AML cells**.

(a) *SYNCRIP* is upregulated in AML patient samples. The graph shows the $\log_2$ expression of *SYNCRIP* from transcriptional profiling of bone marrow cells from patients with various subtypes of AML and of the normal hematopoietic stem/progenitor cells (HSPCs) from healthy donors. AML n=142; AML inv(16)/t(16;16) n=27; AML t(11q23)/MLL n=38; AML ETO n=39; APL n=37; HSC n=8; HPC n=4; Prog n=9; B-cells n=5; Mono n=14; T cell CD4/CD8 n=10. error bars, s.e.m. **** $p<0.0001$ two tailed *t* test. (Hemaexplorer data of *SYNCRIP* probe 209024_s_at from the U133 Plus 2.0 array). (b) SYNCRIP is highly expressed in multiple human AML cell lines. Immunoblot of various myeloid leukemia cell lines compared to cord blood derived CD34+ cells. (c) Primary AML patient samples expressing SYNCRIP. ACTIN serves as loading control. (d–g) Cell proliferation in the indicated cell lines after transduced with lentivirus expressing control or *SYNCRIP*-specific shRNAs. scramble control (black) and two shRNAs (shRNA#1 and #2, blue). n=3 independent experiments per cell line; error bars, s.e.m. ***$p<0.001$ two tailed *t* test. (h) Annexin-V assessed by flow cytometry 24 hours post puromycin selection. n=3 independent experiments per cell line; error bars, s.e.m. * $p<0.05$, **$p<0.001$ two tailed *t* test.
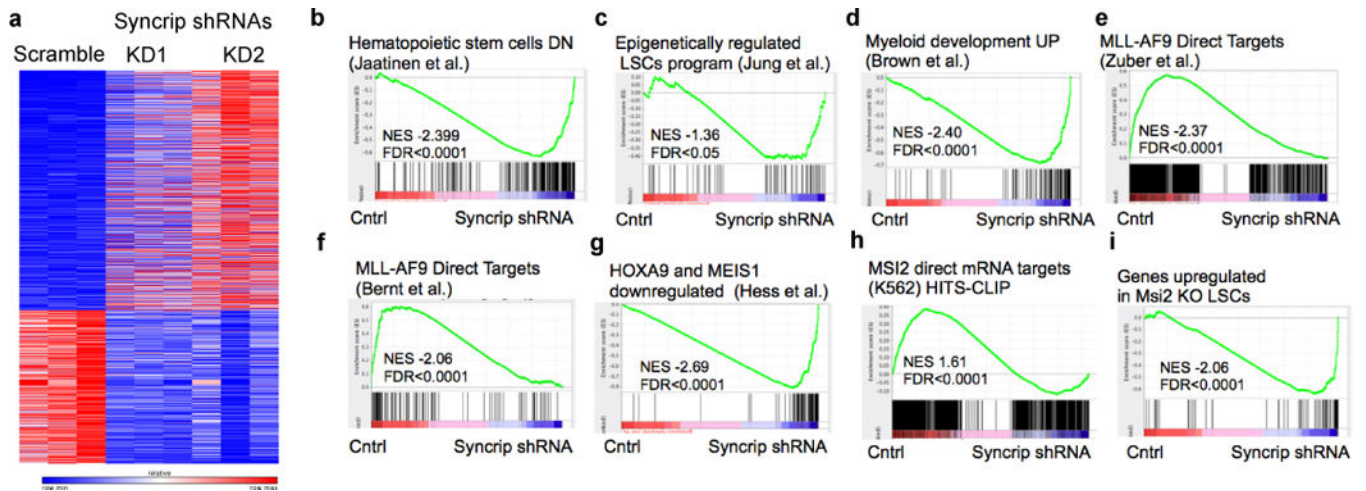
Fig. 5. SYNCRIP regulates the myeloid leukemia stem cell gene expression program
(**a**) Gene expression heat map of the top 191 upregulated and downregulated genes from
RNA-sequencing analysis of MLL-AF9 leukemia cells transduced with control and shRNAs
against *Syncrip.* n=3 biological replicates. (**b–i**) GSEA analysis showing gene expression
signature (**b–c**) genes enriched in hematopoietic stem cells and leukemic stem cells (**d**)
genes upregulated in myeloid development program enriched in *Syncrip*-KD cells (**e–f**)
MLL-AF9 directed taget genes and (**g**) HOXA9-MEIS1 target genes downregulated in
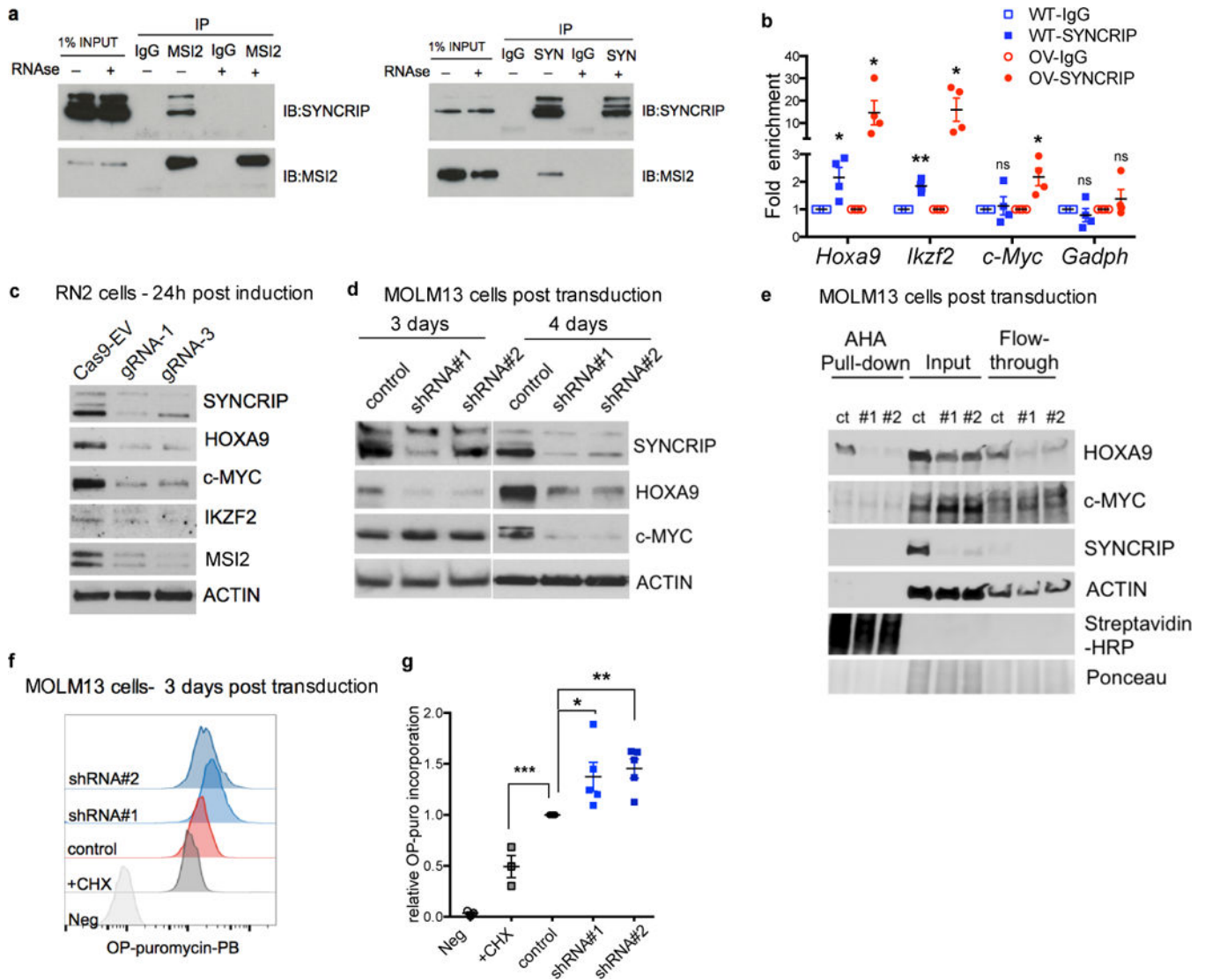*Syncrip*-KD cells (**h–i**) enrichment of MSI2 target genes in SYNCRIP regulated genes.

Fig. 6. SYNCRIP's post-transcriptionally controls HOXA9 protein expression
(**a**) Human myeloid leukemia K562 cells overexpressing MSI2 were immunoprecipated with endogenous MSI2 and SYNCRIP. Lysates incubated with RNase were then immunoprecipated indicating SYNCRIP-MSI2 interaction is RNA mediated. (**b**) SYNCRIP was immunoprecipiated with IgG or SYNCRIP antibody in either endogenous (WT) or human SYNCRIP overexpressing (OV) mouse RN2 MLL-AF9 leukemia cells. n=4 independent experiments; error bars, s.e.m. * p<0.05, **p<0.001 two tailed *t* test. (**c**) Immunoblots showing downregulation of HOXA9, c-MYC and IKZF2 proteins upon SYNCRIP knocked down in RN2 cells. (**d**) Immunoblots showing expression level of HOXA9 and c-MYC upon SYNCRIP-KD in human MOLM13 leukemia cells 3 and 4 days post transduction with viruses expressing control shRNA and SYNCRIP-shRNAs together with GFP. (**e**) Immunoblots showing protein level of SYNCRIP, HOXA9 and c-MYC in AHA-pull down fraction, input and flow through fraction. AHA incorporation into newly synthesized HOXA9 (but not c-MYC) proteins was reduced in SYNCRIP-KD cells. Streptavidin-HRP, Ponceau staining and ACTIN serve as control for total protein input and

loading control. (**f**) Representative histograms analysis of OP-Puro incorporation in control and SYNCRIP-KD MOLM13 cells (shRNA#1 and shRNA#2). (**g**) Quantitative summary of relative OP-Puro incorporation in cells in (**f**). CHX-treated cells were used as negative control (n=3). Cells without OP-Puro incorporation served as staining control. n=4 independent experiments; error bars, s.e.m. *p<0.05, **p<0.001, ***p<0.0001 two tailed *t* test.
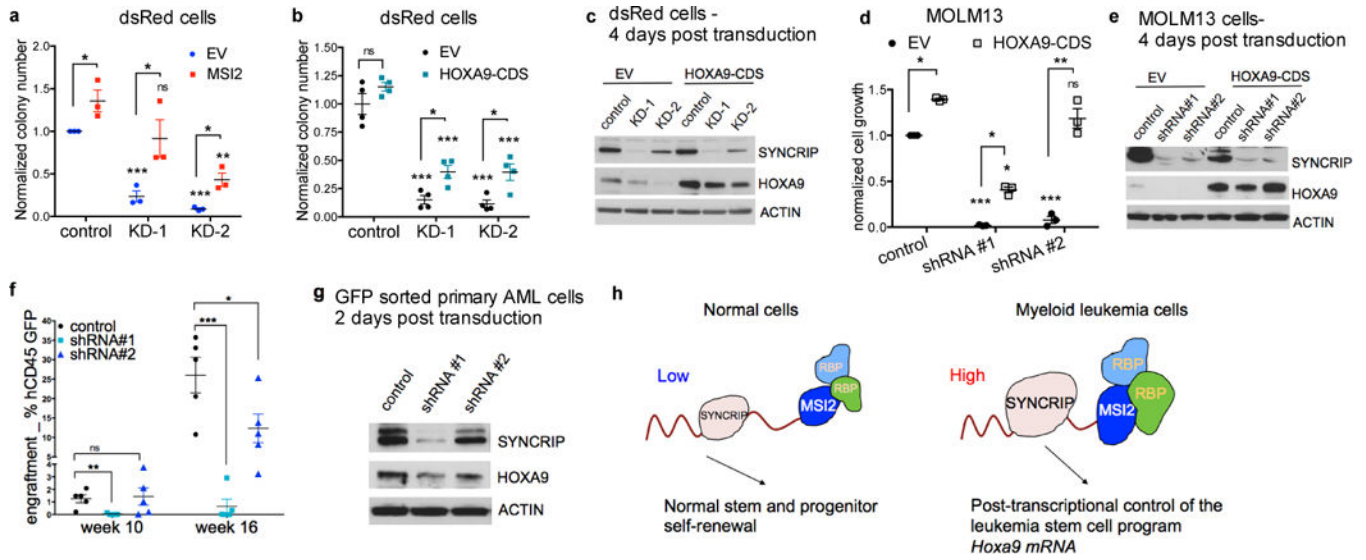
Fig. 7. HOXA9 partially rescues survival defects of SYNCRIP depleted cells

(**a**) Colony formation was rescued in SYNCRIP-KD dsRed leukemia cells with MSI2 overexpression. n=3 independent experiments. (**b**) Colony formation was rescued in dsRed SYNCRIP-KD leukemia cells with HOXA9-CDS overexpression. n=4 independent experiments. (**c**) Immunoblots showing efficient depletion of SYNCRIP expression, protein expression of HOXA9. (**d**) Cell growth was rescued in SYNCRIP-KD human MOLM13 leukemia cells with HOXA9 overexpression. n=3 independent experiments. (**e**) Immunoblots showing efficient depletion of SYNCRIP expression, protein expression of HOXA9. (**f**) Quantitive summary of percentage of engrafted hCD45 GFP cells in recipient mice transplanted with primary AML patient cells transduced with control shRNA or shRNAs against SYNCRIP (shRNA#1 and shRNA#2) at week 10 and week 16 post transplantation. n=5 for each group. (**g**) Immunoblots showing efficient depletion of SYNCRIP expression in primary AML patient cells and downregulation of HOXA9 expression. All data: error bars, s.e.m. ns:*$p<0.05$, **$p<0.001$, ***$p<0.0001$ two tailed t test. (**h**) Schematic depicting the dominant function of SYNCRIP when its expression is elevated in LSCs in comparison to normal HSCs. In LSCs, SYNCRIP and MSI2 binds and increases expression of the mRNA transcripts associated with the MLL self-renewal program, including *Hoxa9* thus driving the LSCs program instead of normal hematopoietic development.